Elastoplastic stress analysis of Nb_3Sn superconducting magnet

Mohammad Reza Vaghar[a)]
National High Magnetic Field Laboratory, University of Florida, Tallahassee, Florida 32306-4005

Hamid Garmestani
Department of Mechanical Engineering and Center for Materials Research and Technology (MARTECH), FAMU/FSU College of Engineering, Tallahassee, Florida 32306-2175

W. Denis Markiewicz
National High Magnetic Field Laboratory, Florida State University, Tallahassee, Florida 32306-4005

(Received 12 July 1995; accepted for publication 13 May 1996)

The plastic behavior of a superconducting material is investigated and the corresponding elastoplastic formulation for the distribution of stress and strain in a superconducting solenoid magnet is presented. The analysis calculates stress and strain at the midsection, where tangential stress exhibits its maximum value and shear stress is negligible. The prediction of stress and strain is essential for both the mechanical and electrical design of high-field superconducting magnets containing Nb_3Sn superconductor. The concept of plasticity is introduced for the first time in the context of magnet design for Nb_3Sn conductor and compared to alternative approaches using conventional elasticity theory. Individual coil sections of a superconducting magnet can be reinforced by an outer section of structural material, the effect of which is included in this formulation. The results show that the elasticity approach using the ''secant modulus method'' does not fully predict the strain distribution; however, it can be used to approximate the stresses. It is shown that for an accurate strain prediction the true nonlinear elastoplastic nature of the superconducting materials should be considered and proper yield criteria should be used. The inaccurate prediction of strains (tangential or radial) can affect critical current density and the evaluation of the reinforcements. © *1996 American Institute of Physics.*
[S0021-8979(96)03616-X]

I. INTRODUCTION

There is a long history of attempts to understand and improve the performance of adiabatically stable, epoxy impregnated superconducting magnets. The tendency of coils to quench prematurely, at relatively low fractions of the critical current, or to exhibit training behavior, in which the coil progressively reaches higher fields in a series of runs, is often attributed to mechanical issues. Frictional motion of the conductor within the windings or of slipping between the windings and adjacent supporting structure can result in heating of the superconductor leading to quench. Stress analysis, and a knowledge of stress, strain, and displacement of the windings, is therefore central to the design of epoxy impregnated superconducting magnets. Lower-field coils usually employ NbTi composite superconductors, which are essentially linear in their stress–strain characteristics to the level of stress typically employed. Higher-field coils commonly employ a Nb_3Sn composite superconductor, in which the Nb_3Sn is formed by a high-temperature heat treatment of the drawn wire. The resulting conductor is significantly nonlinear in its stress–strain characteristics at the usual operating levels of stress. This mechanical behavior motivates an effort to apply plasticity theory to the stress analysis of high-field magnets.

A high-field magnet is often a nested set of individual, mechanically independent coils on separate support structures (Fig. 1). The case of a single constant current density in each coil is assumed here. High-field coils can have additional support structure on the outer diameter to constrain the windings, reducing the level of stress and strain experienced by the conductor. The stress analysis treats one individual coil and its associated reinforcement structure. The total stress in the windings has several sources. Stress is developed during winding of the conductor or possibly during winding of an overbanding support structure. Stress is also developed during the cooling of the magnet to the cryogenic operating temperature due to differences in thermal contraction of the constituent materials. The overriding dominant source of stress is the magnetic stress from the distributed Lorentz force in the windings, and for simplicity is the only stress considered in this analysis.

Previous work has primarily assumed elastic behavior.[1–5] Early analysis, which included a treatment of the external reinforcement structure, assumed only plane stress condition, treating only the dominant tangential and radial stress, and setting the axial stress to zero.[6] This analysis was developed further to include plane stress and plane strain solutions, and providing solutions to the winding and thermal stress as well.[7] A three-dimensional treatment including axial stress and strain, but limited to regions of a coil with zero shear, was presented as a generalized plane strain solution.[8] A detailed plasticity analysis of a cylindrical structure with a body force distribution characteristic of a magnet winding was developed recently[9] and compared to elasticity analysis only for the tangential component.[10] Here the complete formulation of the plasticity analysis as applicable to magnet technology is provided. A comparison between the results of

a)Electronic mail: vaghar@magnet.fsu.edu

 0021-8979/96/80(4)/2490/11/$10.00

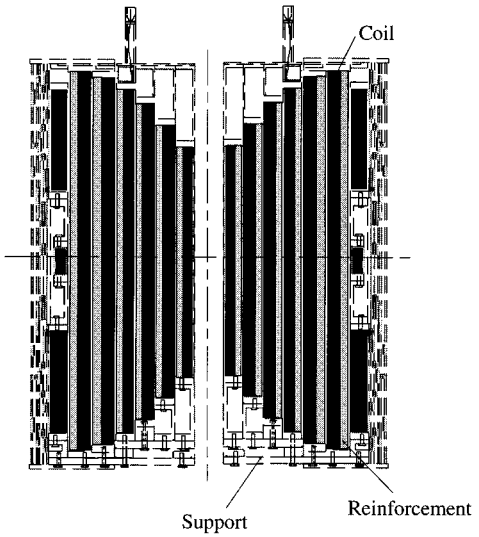

FIG. 1. Schematic diagram of a representative superconducting magnet.

elastic analysis and elastoplastic analysis, and between different assumptions for the yield criteria for the plastic analysis, is presented. This analysis includes the formulation for both tangential and transverse directions.

II. STRESS–STRAIN CURVE

The information required for the application of plasticity theory is contained in the stress–strain curve of a uniaxial tensile test.

The nature of the stress–strain curve of Nb_3Sn composite superconductor is related to the composition and processing of the conductor. The composite superconductor includes a bronze portion around the actual Nb_3Sn filaments, a pure copper stabilizer component, and a small fraction of barrier. This composite conductor is processed at a temperature near 700 °C to form the superconductor. The copper and bronze components are fully annealed. Upon eventual cool down to liquid-helium temperature, thermal differential contraction places the copper in tension, possibly to the point of yield depending on the detailed configuration of the conductor. In the laboratory tensile test, the initial loading force is applied to a composite already in a complex state of internal stress. If the copper stabilizer is close to yield, it is understandable that a limited elastic region is displayed in the stress–strain curve. Eventually the copper and bronze yield, and the nearly linear characteristic displayed by the stress–strain curve at higher levels of stress is related to the Nb_3Sn itself remaining elastic and may partly be a result of work hardening in the copper and bronze. The Nb_3Sn composite conductor is therefore a complex entity which has simultaneous elastic and plastic material components. Such a composite material might be called intrinsically elastoplastic composite. The windings of an adiabatically stable high-field magnet typically combine the Nb_3Sn composite conductor with an epoxy–glass matrix for insulation and support. For the winding composite as a whole, while the conductor may yield at the strain levels under consideration, the epoxy–glass matrix will remain elastic. Thus, on a more macroscopic level, the winding composite of an epoxy impregnated magnet may also be described as an intrinsic elastoplastic composite.

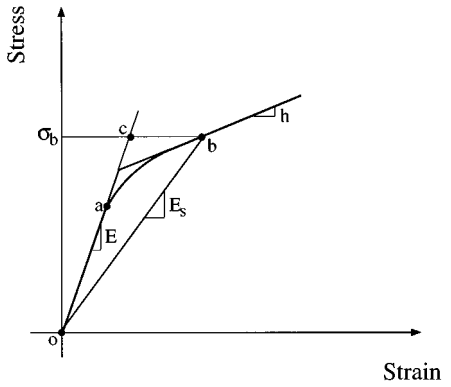

FIG. 2. Stress–strain curve of a typical ductile material.

An idealization of a stress–strain curve obtained for a ductile material is shown in Fig. 2. The plot of applied stress versus total strain usually has an initial linear region in which the material is elastic. As the stress is increased past point a, the stress–strain curve ceases to be linear and the material begins to yield. A simplification will be the use of an elastic linear strain-hardening curve. The initial modulus for the elastic region is E, and the secondary modulus for the plastic region is h. For an approximation of the elastoplastic behavior two alternative elastic paths can be chosen. To reach the stress level σ_b, the oc path with a slope of modulus E can be chosen. It is obvious that this approximation assumes a smaller strain and does not predict the correct state of strain and stress. For this reason another path can be chosen from the origin to point b. The slope of this line is defined as the secant modulus E_s. The secant modulus approach assumes a final state of stress which must be corrected iteratively.

III. FORMULATION OF EQUATIONS

The elasticity formulation of the coil stress analysis is first introduced. One coil of a solenoid is assumed to have inner radius a_1 and outer radius a_2 and a reinforcement at the outside of the coil with outer radius a_3. The coil is made up of elastically orthotropic, linearly work hardening material as shown in Fig. 3, while the reinforcement is a pure elastic material.

The geometry is axisymmetric in nature, and since the body force is present only in the radial direction all shear components are zero. The stress tensor is reduced to three components in the θ, r and z directions. For linear orthotropic elastic material the components of stress and strain are related by Hooke's law,

$$\epsilon_i = \frac{\sigma_i}{E_i} - \sum_{\substack{j=1 \\ j \neq i}}^{3} \nu_{ji} \frac{\sigma_j}{E_j}, \quad i = 1,2,3, \tag{1}$$

where σ_i, ϵ_i, and E_i are stress, strain, and elastic modulus for $i = \theta$, r and z directions and ν_{ij} is Poisson's ratio for i,

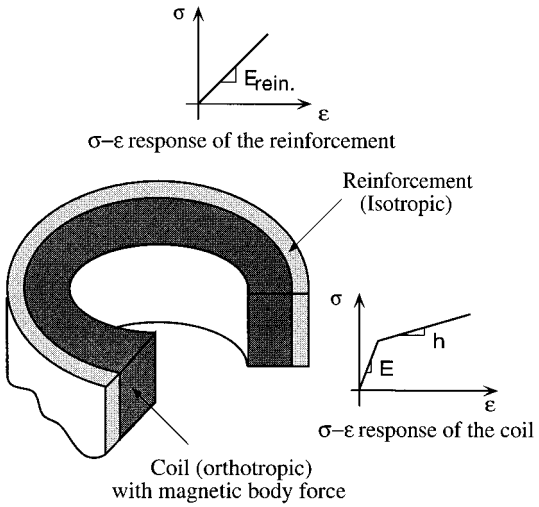

FIG. 3. Schematic diagram representing the two regions of a magnet. The corresponding mechanical behavior is shown as stress–strain curve.

$j=\theta$, r and z $(i\neq j)$. For either plane stress or plane strain assumption, the strain components in θ and r directions reduce to

$$\epsilon_\theta = L\sigma_\theta - V\sigma_r, \quad \epsilon_r = Lk^2\sigma_r - V\sigma_\theta, \tag{2}$$

where for plane stress

$$R=\frac{1}{E_r}, \quad L=\frac{1}{E_\theta}, \quad V=\frac{\nu_{r\theta}}{E_r}=\frac{\nu_{\theta r}}{E_\theta}, \tag{3}$$

and for plane strain

$$R=\frac{1-\nu_{rz}\nu_{zr}}{E_r},$$

$$L=\frac{1-\nu_{\theta z}\nu_{z\theta}}{E_\theta}, \tag{4}$$

$$V=\frac{\nu_{r\theta}+\nu_{z\theta}\nu_{rz}}{E_r}=\frac{\nu_{\theta r}+\nu_{\theta z}\nu_{zr}}{E_\theta},$$

and for both plane stress and plane strain

$$k=\left(\frac{R}{L}\right)^{1/2}. \tag{5}$$

The factor k defines the mechanical anisotropy of elastic moduli in the $r-\theta$ plane.

Strains are related to the displacement according to the following relations:

$$\epsilon_r=\frac{du}{dr}, \quad \epsilon_\theta=\frac{u}{r}, \tag{6}$$

where u is the displacement in the radial (r) direction.

For an axisymmetric solenoid the equilibrium equations reduce to

$$\frac{d\sigma_r}{dr}+\frac{\sigma_r-\sigma_\theta}{r}+X_r=0, \tag{7}$$

where X_r is the body force. Magnetic body force is directly proportional to the product of current density and magnetic field. In this article the stress analysis is performed for the midsection of the solenoid, in which case the magnetic field can be approximated as a linear function of radius,

$$B_z=J(\alpha-\beta r), \tag{8}$$

where J is the current density and α and β are arbitrary constants which can be determined from the current density and the boundary conditions specified for the field. The current density J is assumed to be constant through each single coil; therefore, the magnetic body force is a linear function of radius,

$$X_r=JB_z=J^2(\alpha-\beta r). \tag{9}$$

Equilibrium equation is then reduced to the following:

$$\frac{d\sigma_r}{dr}+\frac{\sigma_r-\sigma_\theta}{r}+J^2(\alpha-\beta r)=0. \tag{10}$$

By substituting Eq. (6) into Eq. (2) stresses are calculated in terms of displacements. Substituting the stresses into Eq. (10) and with the plane stress or strain assumption a differential equation for the radial displacement can be obtained,

$$u''+\frac{u'}{r}-k^2\frac{u}{r^2}=-J^2(\alpha-\beta r)\frac{L^2k-V^2}{L}. \tag{11}$$

The solution to this differential equation gives the displacement,

$$u=(L^2k^2-V^2)\left[\frac{c_1}{Lk+V}r^k+\frac{c_2}{Lk-V}r^{-k} - \frac{J^2}{L}\left(\frac{\alpha}{4-k^2}r^2-\frac{\beta}{9-k^2}r^3\right)\right], \tag{12}$$

and hence the stresses in the elastic region,

$$\sigma_r=c_1r^{k-1}+c_2r^{-k-1}+J^2S_1r+J^2S_2r^2,$$
$$\sigma_\theta=c_1kr^{k-1}-c_2kr^{-k-1}+J^2T_1r+J^2T_2r^2, \tag{13}$$

where c_1 and c_2 are arbitrary constants; S_1, S_2, T_1, and T_2 are constants calculated from the mechanical properties and magnetic fields of the coil,

$$S_1=-\left(2+\frac{V}{L}\right)\frac{\alpha}{4-k^2}, \quad S_2=\left(3+\frac{V}{L}\right)\frac{\beta}{9-k^2},$$
$$T_1=-\left(k^2+\frac{2V}{L}\right)\frac{\alpha}{4-k^2}, \quad T_2=\left(k^2+\frac{3V}{L}\right)\frac{\beta}{9-k^2}. \tag{14}$$

The theory of plasticity is formulated in terms of flow rules which give the increments of plastic strain in terms of

applied stress. The flow rule is a description of the yielding process in the material, and as such is dependent on the yield criterion or yield function for the material. The flow rules associated with the yield functions of von Mises, Tresca, and Hill are used to derive equations for the stresses in the superconducting magnets.

A. von Mises yield criterion

For the well-known von Mises yield criterion, the flow rule relates the increments of plastic strain $d\epsilon_{ij}^p$ to the components of the deviator stress tensor $S_{ij}=\sigma_{ij}-\frac{1}{3}\sigma_{kk}\delta_{ij}$,

$$d\epsilon_{ij}^p=\frac{3}{2}\frac{d\epsilon^p}{\sigma_e}S_{ij}. \tag{15}$$

The effective stress σ_e has the form of the von Mises yield function, which in the absence of shear stress reduces to

$$\sigma_e^2=\tfrac{1}{2}[(\sigma_\theta-\sigma_z)^2+(\sigma_z-\sigma_r)^2+(\sigma_r-\sigma_\theta)^2]. \tag{16}$$

For the plane strain condition, assuming the von Mises yield function, a closed-form solution can be derived for the tangential and radial components of stress and strain. Essential to the derivation is the observation that for the plane strain condition the plastic increment of the axial strain $d\epsilon_z^p$ becomes zero. Using Eq. (15) it is obvious that the deviatoric stress in the corresponding direction z must be zero. The axial stress can then be calculated from

$$\sigma_z=\tfrac{1}{2}(\sigma_r+\sigma_\theta), \tag{17}$$

therefore, the components of the deviator stress tensor are simply proportional to the effective stress. By substituting Eq. (17) into Eq. (16) the von Mises yield criterion reduces to

$$\sigma_\theta-\sigma_r=\frac{2}{\sqrt{3}}\sigma_e. \tag{18}$$

The flow rule is then integrated directly to give an algebraic relation between the plastic strain components and the effective strain which is independent of the stresses,

$$\epsilon_\theta^p=-\epsilon_r^p=\frac{\sqrt{3}}{2}\epsilon^p. \tag{19}$$

B. Tresca yield criterion

For the Tresca yield criterion, flow rule has the form of

$$d\epsilon_{ij}^p=2d\epsilon^p\frac{\partial f(\sigma_{ij})}{\partial\sigma_{ij}}, \tag{20}$$

which relates the increments of plastic strain components $d\epsilon_{ij}^p$ to increments of effective plastic strain $d\epsilon^p$ and partial derivatives of yield function $f(\sigma_{ij})$ with respect to stress components σ_{ij}. The Tresca yield function has the form of

$$f(\sigma_{ij})\equiv\tfrac{1}{2}(\sigma_{\max}-\sigma_{\min})=\tfrac{1}{2}\sigma_e. \tag{21}$$

For the case of plane stress, the tangential stress (σ_θ) is a maximum and radial stress (σ_r) is a minimum ($\sigma_\theta>0>\sigma_r$). For plane strain, the axial stress (σ_z) is always less than tangential stress ($\sigma_\theta>\sigma_z>0>\sigma_r$). Thus, the Tresca yield criterion reduces to the simple form of

$$f(\sigma_{ij})\equiv\tfrac{1}{2}(\sigma_\theta-\sigma_r)=\tfrac{1}{2}\sigma_e. \tag{22}$$

Differentiating the Tresca yield function with respect to the stress components, and using the flow rule, plastic strains are found in terms of effective plastic strain,

$$\epsilon_\theta^p=-\epsilon_r^p=\epsilon^p. \tag{23}$$

It can be seen that the two yield criteria for the case of plane strain are derived from very similar formulations and hence both are treated here at the same time.

An elastic linear strain-hardening constitutive relation is used to represent the stress–strain history in the plastic region. For such a material the relationship between the effective plastic strain and effective stress is

$$\sigma_e=\sigma_Y+c\epsilon^p, \tag{24}$$

where σ_e is the effective stress, σ_Y is the yield stress for uniaxial tensile test, ϵ^p is the effective plastic strain, and c is a parameter which can be calculated from the initial modulus E and the secondary modulus for the plastic region h,

$$c=\frac{Eh}{E-h}. \tag{25}$$

From the strain-displacement relationships, Eq. (6), the compatibility equation is defined as

$$\frac{d\epsilon_\theta}{dr}=\frac{\epsilon_r-\epsilon_\theta}{r}, \tag{26}$$

where strains are the total strains. In the plastic region the total strain is a combination of elastic and plastic strains,

$$\epsilon_r=\epsilon_r^e+\epsilon_r^p,\quad \epsilon_\theta=\epsilon_\theta^e+\epsilon_\theta^p, \tag{27}$$

where ϵ_i^e and ϵ_i^p stand for elastic and plastic strain.

By substituting Eq. (27) into Eq. (26), the compatibility equation reduces to

$$\frac{d\epsilon_\theta^p}{dr}+\frac{\epsilon_\theta^p-\epsilon_r^p}{r}+\frac{d\epsilon_\theta^e}{dr}+\frac{\epsilon_\theta^e-\epsilon_r^e}{r}=0. \tag{28}$$

Rewriting Eq. (28), using Eqs. (2), (10), (18), (19), (22), (23), and (24), a unified differential equation can be obtained,

$$F_1\frac{d\epsilon_\theta^p}{dr}+2F_1\frac{\epsilon_\theta^p}{r}+F_2\frac{1}{r}\int\frac{\epsilon_\theta^p}{r}dr+F_3\frac{1}{r}+F_4\frac{\ln r}{r}+J^2F_5+J^2F_6r=0, \tag{29}$$

where F_1 through F_6 are

$$F_1=1+\zeta^2 Lc, \quad F_2=\zeta^2 Lc(1-k^2),$$

$$F_3=2\zeta L\sigma_Y, \quad F_4=\zeta L(1-k^2)\sigma_Y, \tag{30}$$

$$F_5=-[(L-V)+L(1-k^2)]\alpha,$$

$$F_6=\left[(L-V)+\frac{L}{2}(1-k^2)\right]\beta,$$

and where ζ represents a yield parameter which is one for Tresca and $2/\sqrt{3}$ for von Mises.

It should be noted that the same equations are valid for the case of plane stress for the Tresca criterion, with the associated definition of R, V, and L according to Eq. (3).

Solution of the differential Eq. (29) provides ϵ_θ^p,

$$\epsilon_\theta^p=c_3 n_1 r^{n_1}+c_4 n_2 r^{n_2}+J^2 H_1 r+J^2 H_2 r^2+H_3, \tag{31}$$

TABLE I. Parameters for example coil.

Name	Symbol	Value	Unit
Inner radius[a]	a_1	14.50	cm
Outer radius[a]	a_2	17.70	cm
Outer radius[b]	a_3	18.40	cm
Young modulus in tangential direction[a]	E_θ	105.00	GPa
Young modulus in radial direction[a]	E_r	35.00	GPa
Young modulus[b]	$E_{\text{rein.}}$	200.00	GPa
Yield stress[a]	σ_Y	75.00	MPa
Internal pressure	P_i	0.00	MPa
Poisson ratio[a]	$\nu_{\theta r}$	0.25	
Poisson ratio[b]	$\nu_{\text{rein.}}$	0.30	
Magnetic field at inner radius[a]	B_1	14.50	T
Magnetic field at outer radius[a]	B_2	10.00	T
Current density[a]	J	113.00	A/mm^2
Secondary plastic modulus[a]	h	21.00	GPa
Secant modulus in tangential direction[a]	$E_{s\theta}$	45.00	GPa
Secant modulus in radial direction[a]	E_{sr}	15.00	GPa

[a]For coil.
[b]For reinforcement.

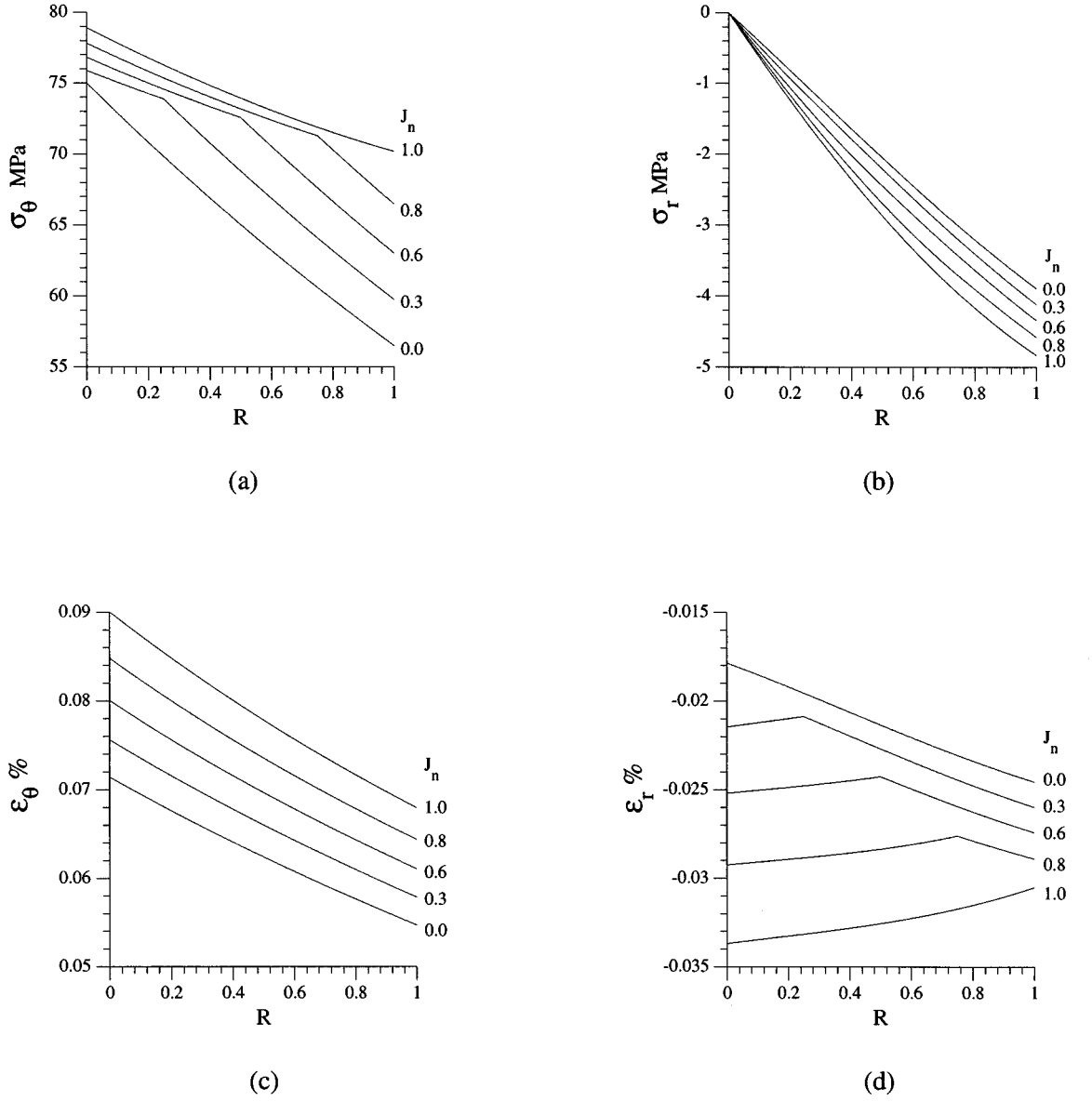

FIG. 4. Plane stress analysis using Tresca yield criterion: (a) tangential stress; (b) radial stress; (c) tangential strain; and (d) radial strain.

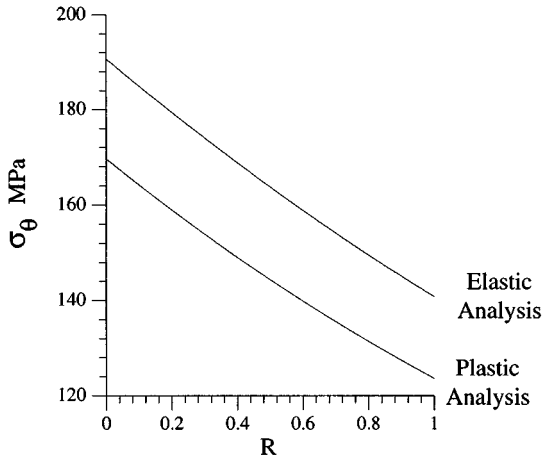

(a)

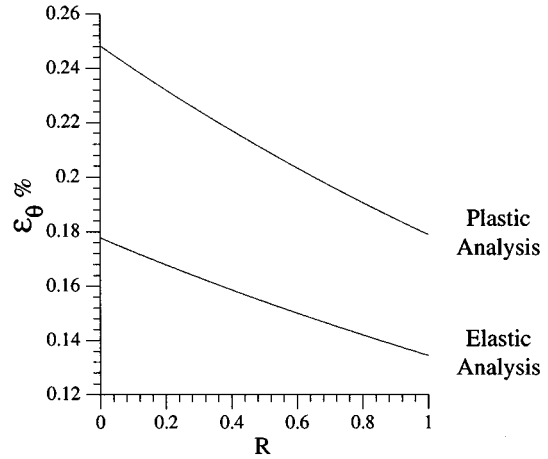

(b)

FIG. 5. Deviation from elastic analysis for the same loading conditions. The plastic analysis is performed using Tresca yield criterion and plane strain assumption: (a) tangential stress and (b) tangential strain.

where c_3 and c_4 are arbitrary constants that can be determined from the boundary conditions and H_1 through H_4, and n_1, and n_2 are constants,

$$H_1=\frac{[(L-V)+L(1-k^2)]\alpha}{3+\zeta^2 Lc(4-k^2)},$$

$$H_2=\frac{-2[(L-V)+(L/2)(1-k^2)]\beta}{8+\zeta^2 Lc(9-k^2)},$$

$$H_3=-\frac{1}{\zeta c}\,\sigma_Y,\quad H_4=\frac{2}{\zeta^3 Lc^2(1-k^2)}\,\sigma_Y, \tag{32}$$

$$n_1=-1+\left(\frac{1+\zeta^2 Lck^2}{1+\zeta^2 Lc}\right)^{1/2},$$

$$n_2=-1-\left(\frac{1+\zeta^2 Lck^2}{1+\zeta^2 Lc}\right)^{1/2}.$$

From Eq. (31) the stresses in the plastic region are

$$\begin{aligned}\sigma_r&=\zeta^2 c(c_3 r^{n_1}+c_4 r^{n_2})+J^2 S_3 r+J^2 S_4 r^2+S_5\ln r+S_6,\\ \sigma_\theta&=\zeta^2 c[c_3(1+n_1)r^{n_1}+c_4(1+n_2)r^{n_2}]+J^2 T_3 r\\ &\quad+J^2 T_4 r^2+T_5\ln r+T_6,\end{aligned} \tag{33}$$

where S_3 through S_6 and T_3 through T_6 are constants,

$$\begin{aligned}&S_3=\zeta^2 cH_1-\alpha,\quad S_4=\tfrac{1}{2}(c\zeta^2 H_2+\beta),\\ &S_5=\zeta^2 cH_3+\zeta\sigma_Y,\quad S_6=\zeta^2 cH_4,\\ &T_3=\zeta^2 cH_1+S_3,\quad T_4=\zeta^2 cH_2+S_4,\\ &T_5=S_5,\quad T_6=\zeta^2 cH_3+S_6+\zeta\sigma_Y.\end{aligned} \tag{34}$$

For the plane stress assumption with the von Mises yield function, a closed-form solution cannot be obtained. This situation is described for a more general case of Hill's criterion below.

C. Hill's yield criterion

For an orthotropic material, the von Mises yield function is generalized to Hill's orthotropic yield function which in the principal magnet coordinates is written

$$f(\sigma_{ij})\equiv\tfrac{1}{2}[F(\sigma_\theta-\sigma_r)^2+G(\sigma_r-\sigma_z)^2+H(\sigma_z-\sigma_\theta)^2]=\tfrac{1}{2}, \tag{35}$$

where F, G, and H are related to the tensile yield stresses in the principal directions. An epoxy impregnated magnet winding is nearly transversely isotropic, and this assumption is used in the following. For a transversely isotropic material ($F=H$), Hill's function reduces to

$$\sigma_e^2=\tfrac{1}{2}[(\sigma_\theta-\sigma_r)^2+\eta(\sigma_r-\sigma_z)^2+(\sigma_z-\sigma_\theta)^2]. \tag{36}$$

Note that the effective yield stress is equal to the tangential yield stress for a uniaxial tensile test. The parameter η is a measure of anisotropy and may be written as

$$\eta=\frac{G}{F}=2\left(\frac{\sigma_{y\theta}}{\sigma_{yr}}\right)^2-1, \tag{37}$$

where $\sigma_{y\theta}$ and σ_{yr} are yield stresses in tangential and radial directions.

The more general formulation of plasticity is based on a flow rule of the form

$$d\epsilon_{ij}^p=d\lambda\,\frac{\partial f(\sigma_{ij})}{\partial\sigma_{ij}}, \tag{38}$$

where the increments of plastic strain are related through the scalar differential quantity ($d\lambda$) to the derivatives of the

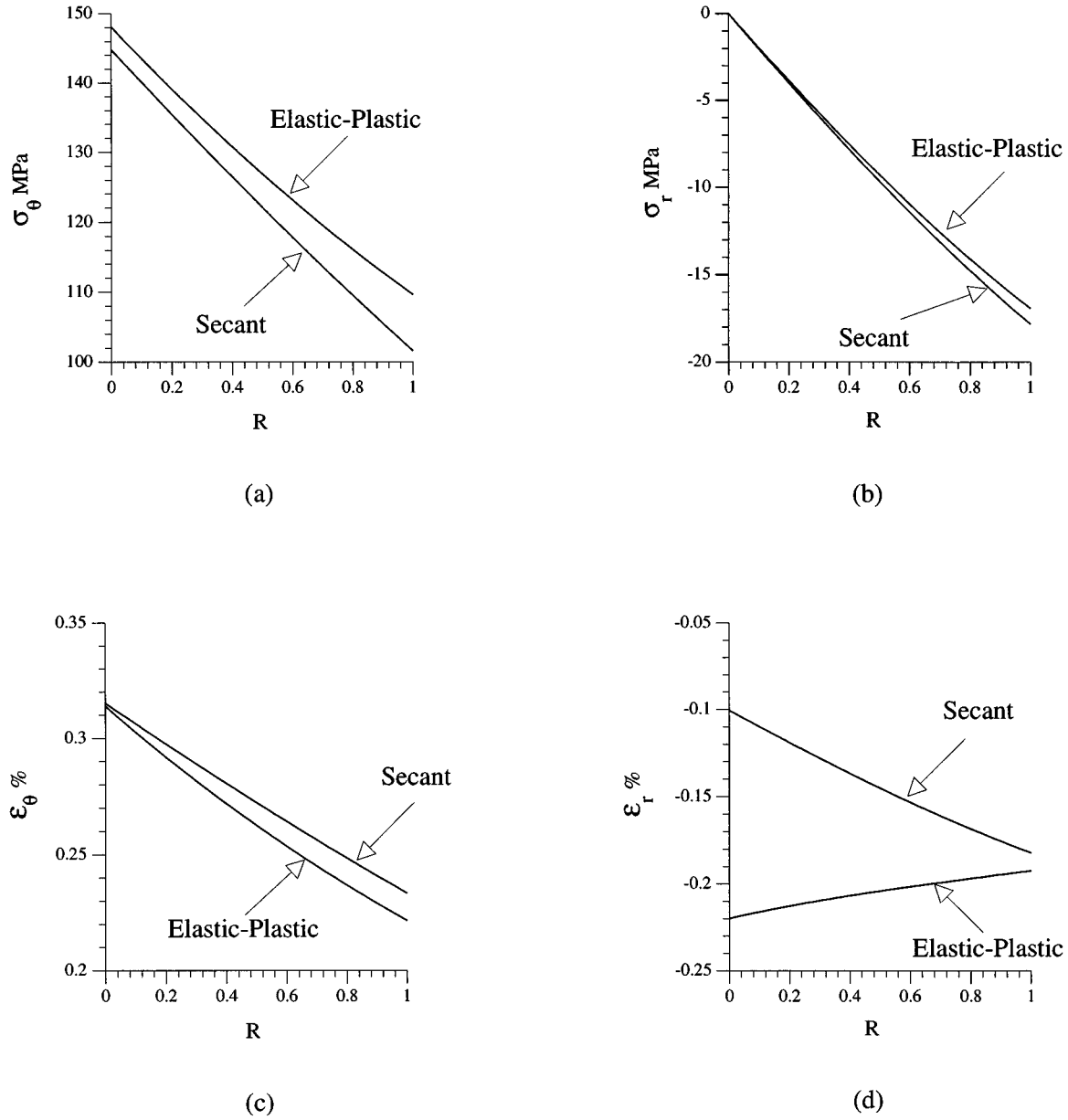

FIG. 6. Comparison between secant and elastic–plastic (von Mises) analysis for plane strain condition: (a) tangential stress; (b) radial stress; (c) tangential strain; and (d) radial strain.

yield function. The flow rule for the transversely isotropic material is then obtained by substituting the yield function into the general form of the flow rule.

Using the proportional loading condition, the differential form of the flow rule may be integrated directly to give an algebraic equation for the plastic strain components. It is possible to use Hooke's law, the equilibrium equation, and the constitutive equation to eliminate strains and arrive at two coupled nonlinear first-order differential equations for the two components of stress,

$$\frac{d\sigma_\theta}{dr}=F_1(\sigma_\theta,\sigma_r), \quad \frac{d\sigma_r}{dr}=F_2(\sigma_\theta,\sigma_r). \tag{39}$$

These differential equations are solved using a numerical scheme.[9]

IV. RESULTS AND DISCUSSION

The elastoplastic analysis is investigated for a Nb_3Sn superconducting coil with reinforcement. The parameters of the coil and reinforcement are presented in Table I. Calculations were made using elastoplastic theory with von Mises, Tresca, and Hill's yield criteria. These results are compared with that of the elasticity theory using the secant modulus. Equations (33) (for plastic region) and (13) (for elastic region) are used to calculate stresses based on elastoplastic analysis and Eq. (13) is used to calculate stresses based on elastic analysis. Equation (39) is used to calculate the stresses numerically based on the plastic analysis and Hill's (orthotropic) yield criterion. Once the stresses are calculated, strains can be determined separately for the elastic and plastic regions.

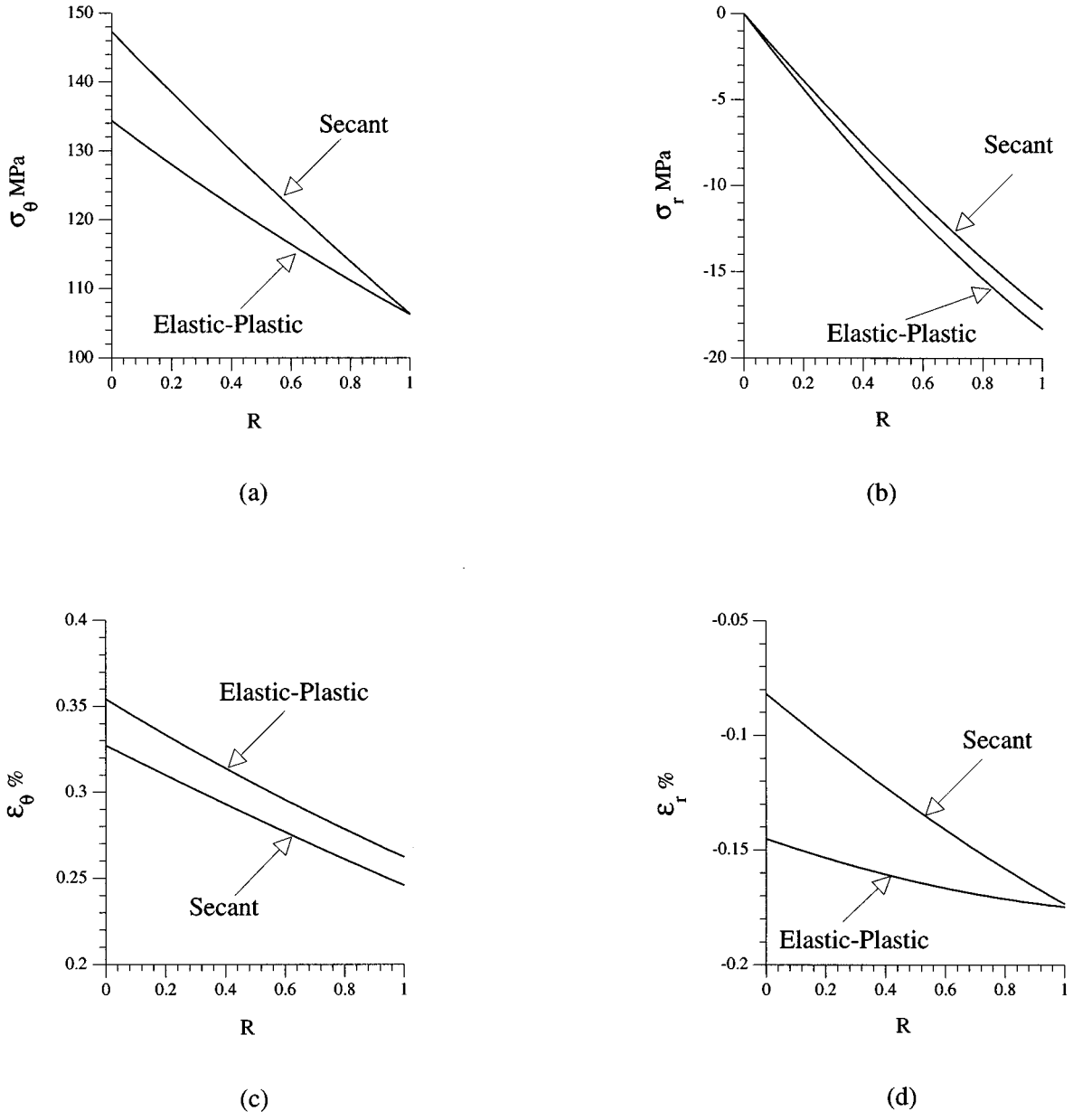

FIG. 7. Comparison between secant and elastic–plastic (von Mises) analysis for plane stress condition: (a) tangential stress; (b) radial stress; (c) tangential strain; and (d) radial strain.

To present the results two normalized parameters R and J_n are defined such that for the fully elastic case at the onset of yielding, J_n becomes zero and for the fully plastic case J_n becomes equal to one. In this formulation the two boundaries $R=0$ and 1 refer to inner and outer radii (a_1, a_2),

$$R=\frac{r-a_1}{a_2-a_1}, \quad J_n=\frac{J-J_y}{J_p-J_y}. \tag{40}$$

Here J_y is the current density at the onset of yielding (at the inner radius) and J_p is the current density for complete plasticity.

Figure 4 presents a parametric study which includes the effect of plasticity on the distribution of the two components of stress and strain. The effect of plasticity and its spread is examined for different values of current density J. Since there is a direct correlation between the current density and the resulting magnetic body forces, J (hence J_n) can be assumed to be a controlling parameter in this study.

Figure 5 shows a comparison between the elastic analysis using the original elastic modulus E and the elastoplastic case. The analysis is performed to a current density at which the material becomes fully plastic. The results show a large error in the values obtained for the tangential strain (an error of about 30%). For this reason we limit our analysis to the case of secant modulus and its comparison to elastoplastic analysis.

Figs. 6 and 7 show the distribution of stresses and strains through the coil with plane strain and plane stress conditions for two cases of elastic analysis using the secant modulus and elastoplastic analysis. Results show similar behavior for

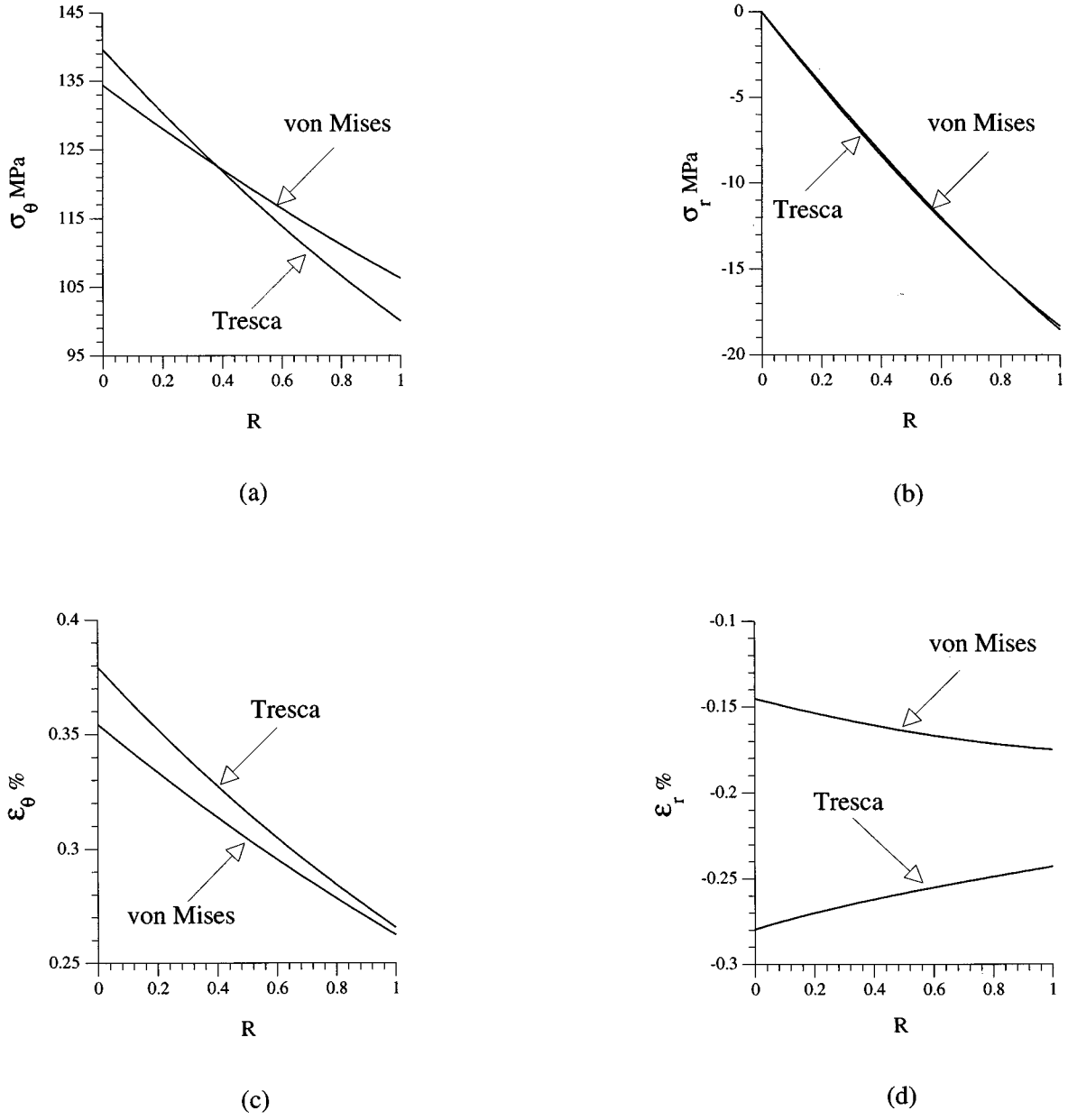

FIG. 8. Comparison between Tresca and von Mises yield criterion for plane stress condition: (a) tangential stress; (b) radial stress; (c) tangential strain; and (b) radial strain.

σ_θ with a difference of less than 10%. Radial stress (σ_r) distribution shows an even smaller difference.

The results of the analysis for the tangential strain distribution show a difference of about 10% for the plane stress condition [Fig. 7(c)]. This difference is not only an error in predicting the mechanical strain, but can also influence the electrical performance of the magnet because the critical current density is strain sensitive. The difference in radial strain is dramatically larger [Figs. 6(d) and 7(d)] and it behaves quite different in the elastoplastic analysis compared to that of elastic analysis.

A comparison is performed between the two yield criteria for the case of plane stress. Figure 8 shows the stresses and strains for the von Mises and Tresca yield criteria. The results show that the difference for the stresses [Figs. 8(a) and 8(b)] and tangential strain [Fig. 8(c)] is small; however, the results for the radial strain show a large difference [Fig. 8(d)].

The above calculations were performed assuming an isotropic yield stress in the windings. The implications of an orthotropic yield criterion are shown in Fig. 9, where Hill's yield criterion is used for a range of values of η in Eq. (37). Anisotropy ($\eta>1$) in general results in a decrease in the distribution of radial stress and an increase in the distribution of tangential stress [Figs. 9(a) and 9(b)]. The material studied is transversely isotropic and has a low modulus in transverse direction (radial and axial). This results in a decrease in the value of the radial stress. Both components of strain (radial and tangential) decrease in their magnitude as the material becomes more anisotropic [Figs. 9(c) and 9(d)]. The analysis

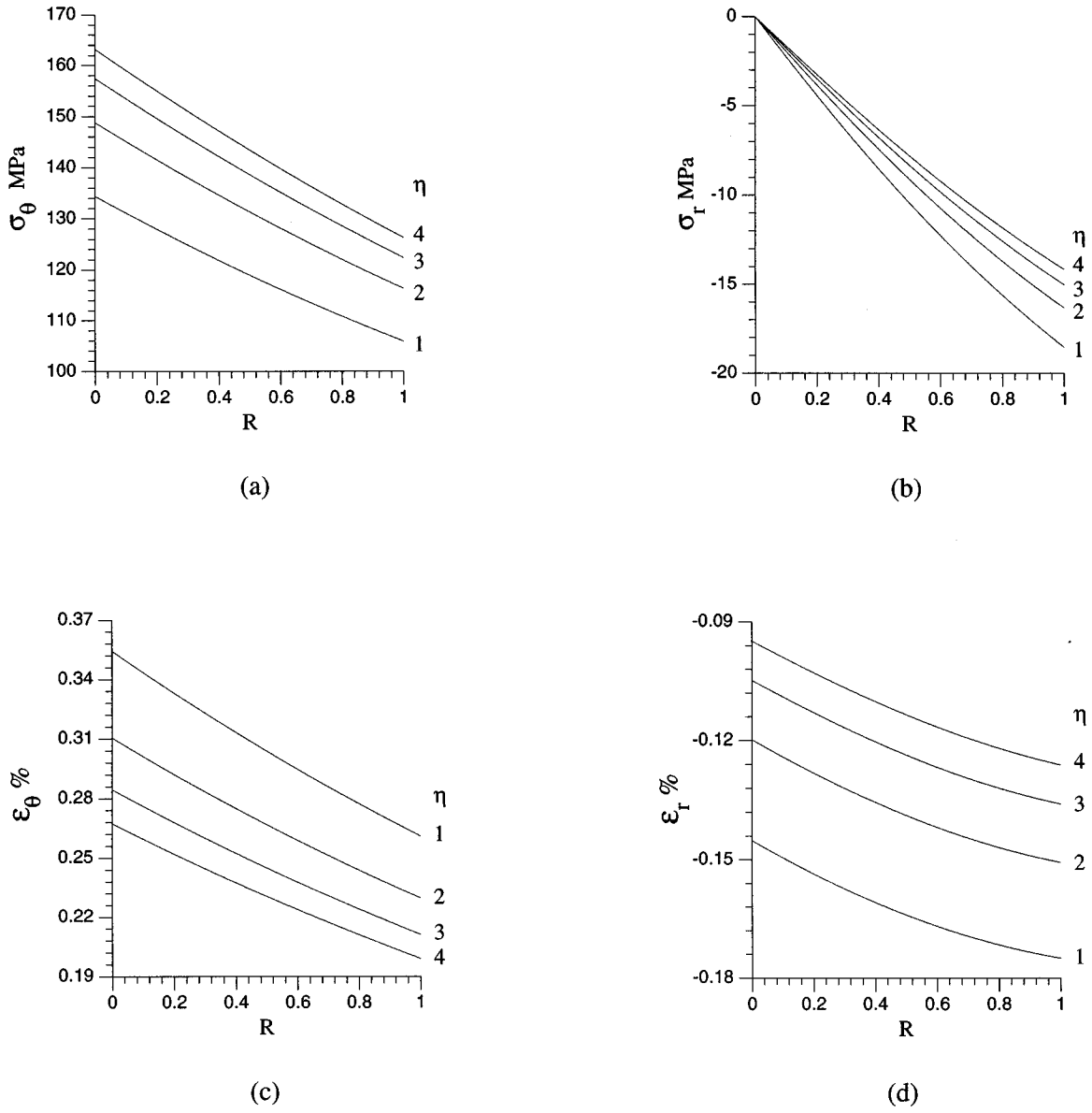

FIG. 9. Plane stress analysis using Hill's yield criterion for completely plastic: (a) tangential stress; (b) radial stress; (c) tangential strain; and (d) radial strain.

also shows a 20% difference in predicted tangential stress between the case of isotropy, for which $\eta=1$, and the anisotropic case for which $\eta=4$.

V. CONCLUSION

Classical plasticity theory together with related yield criteria including Hill's orthotropic yield function is reviewed and a complete elastoplastic analysis is performed for the Nb_3Sn superconducting coil. The results are compared to elastic solutions based on the elastic modulus E and an alternative secant modulus E_s. This analysis shows that the elastic solution based on elastic modulus cannot produce a correct state of stress and strain. Elastic solution based on secant modulus provides the stress state with minimal error; however, it cannot be used to calculate the strain. Furthermore, the determination of the secant modulus requires a process of trial and error whereas the elastoplastic analysis explores the true nature of the stress–strain curve, and once implemented the stress state can be predicted with no further assumptions.

This work produced the formulation based on classical rate independent plasticity. Further work should seek solutions which include the effect of strain rate in a unified inelastic formulation. Additional experimental data is needed for the constants required in the implementation of the Hill's yield criterion such that the theory can be fully exploited.

[1] D. Montgomery, *Solenoid Magnet Design* (Wiley-Interscience, New York, 1969).
[2] H. Burkhard, J. Appl. Phys. **6**, 357 (1975).
[3] H. Brechna, *Superconducting Magnet Systems* (Springer, New York, 1973).
[4] S. Lekhnitskii, *Theory of Elasticity of an Anisotropic Elastic Body* (Holden-Day, San Francisco, 1963).
[5] L. Calcote, *Introduction to Continuum Mechanics* (Van Nostrand, New York, 1969).

[6] L. Calcote, *Introduction to Continuum Mechanics* (Van Nostrand, New York, 1969).
[7] L. M. Lontai and P. G. Marston, in Proceedings of the International Symposium on Magnet Technology, Stanford University, CA, 1965, pp. 723–732.
[8] V. Arp, J. Appl. Phys. **48**, 2026 (1977).
[9] W. D. Markiewicz, M. R. Vaghar, I. R. Dixon, and H. Garmestani, IEEE Trans. Magn. **MAG-30**, 2233 (1994).
[10] H. Garmestani, M. R. Vaghar, W. Markiewicz, and N. Chandra, Int. J. Mech. Struct. Machines **23**, 521 (1995).
[11] H. Garmestani, M. R. Vaghar, and W. Markiewicz, IEEE Trans. Magn. **MAG-30**, 2237 (1994).